Geomechanics for Energy and the Environment 22 (2020) 100179

Contents lists available at ScienceDirect

Geomechanics for Energy and the Environment

journal homepage: www.elsevier.com/locate/gete

Investigating effects of temperature and confining pressure on dynamic elastic properties and permeability—An experimental study

Mahdi Ramezanian *, Hossein Emadi

Texas Tech University, 2500 Broadway, Lubbock, TX 79409, USA

ARTICLE INFO

Article history:
Received 22 August 2019
Received in revised form 21 November 2019
Accepted 6 January 2020
Available online 13 January 2020

Keywords:
Unconventional reservoirs
Permeability
Temperature
Dynamic elastic properties

ABSTRACT

Unconventional reservoirs refer to hydrocarbon reservoirs that require special stimulation treatments, such as hydraulic fracturing, to economically produce hydrocarbon. These reservoirs are tight with very low permeability, less than 0.1 milli Darcy (0.1 mD). Shale oil and shale gas reservoirs are prime examples of unconventional reservoirs. Effects of temperature on unconventional reservoirs' dynamic elastic properties and permeability are usually overlooked during laboratory measurements and reservoir simulations leading to erroneous results and unsuccessful stimulation operations.

To investigate effects of temperature and confining pressure on dynamic elastic properties and permeability of unconventional core samples, two series of experiment were conducted on outcrop core samples from three prominent unconventional basins (Barnett, Wolfcamp, and Eagle Ford) in the United States. In the first set of experiments, eleven unsaturated outcrop core samples (four Barnett, four Eagle Ford, and three Wolfcamp) were used to assess effects of temperature and confining pressure on their dynamic elastic properties. In the second set of the experiments, seven core samples (two Barnett, two Eagle Ford, and three Wolfcamp) were used to study effect of temperature on their permeability at a constant confining pressure. Also, X-ray diffraction (XRD) analysis was conducted on core samples to determine the mineral compositions them. The results were then used to study effect of mineralogy on the rock samples' dynamic elastic properties and permeability.

The results of this experimental study show that increase in temperature makes the core samples more ductile and less permeable. The results also demonstrate that the degree of the effect of the temperature on the dynamic elastic properties of the samples is directly related to the presence and volume of the clay minerals.

1. Introduction

Development of unconventional hydrocarbon resources has been accelerated in the last decade with the emergence of several innovations in tools and improvements in development methods that enhance hydrocarbon production. Consequently, shale formations have been extensively studied worldwide to obtain a better understanding of their characteristics and behaviors under various circumstances. Numerous laboratory and simulation studies have been conducted on shale rock samples to investigate their mechanical properties and failure mechanisms and the results are used to improve drilling and stimulation operations.[1,2] Although several studies demonstrated that rock properties drastically change with temperature and confining pressure, most of the rock property measurements are conducted at ambient conditions. The outcomes of these studies are wrongly used to predict the rock behavior and failure in downhole conditions, which yields to erroneous results. Extensive studies have been conducted on rock samples, mainly granite, to investigate effects of high temperature and thermal cycling on their mechanical properties in geothermal reservoirs. But effects of temperature on mechanical properties and permeability of unconventional formations have not been thoroughly investigated. Formation temperatures are not constant during the lifespan of a wellbore. For example, injecting steam into a reservoir increases the formation temperature and alters its mechanical properties. On the other hand, water flooding and hydraulic fracturing treatment reduce formation temperatures. Changes in in-situ stress conditions and temperature alter a rock sample's mechanical properties and permeability. Increase in confining pressure applied on a core sample results in compacting the sample and permeability reduction. Permeability also decreases at elevated temperatures because of matrix expansion and closure of existing micro-cracks.[3–5] Changes in temperature and confining pressure result in rock elastic moduli alterations.[4,6,7] Strain, rock resistivity, compressibility, compressional and shear wave velocities, density, and unconfined compressive strength are other properties that are affected by temperature and confining pressure.[3]

* Corresponding author.
E-mail address: mahdi.ramezanian@ttu.edu (M. Ramezanian).

https://doi.org/10.1016/j.gete.2020.100179
2352-3808/

Results of experimental studies conducted on Toarcian source rock samples revealed that increase in temperature and confining pressure increased ductility of the samples.[8–10] Increase in temperature results in thermal damage of the rock matrix that may alter the porosities of the samples.[11] Increasing the temperature causes different types of failures in granite, which consequently altered the rock mechanical properties.[12] In most simulation and experimental studies, stresses and pressures are the only parameters considered to predict a rock behavior in downhole conditions. Effects of temperature on rock mechanical properties that could be significant are usually ignored in these studies. Cooling down a formation and applying thermal shock increase the porosity and tensile strength of the rocks in geothermal reservoirs.[13] Results of a numerical modeling demonstrate that injecting cold fluid results in an increase in fracture volume and width compared to the regular fracturing treatment using ambient temperature fluid at the same downhole conditions.[14] Injecting cold fluid into a core sample results in applying tensile stress on the sample causing rock contraction yielding creation of small fractures in the sample. Positive effects of thermally induced microcracks on enhancing oil and gas production from unconventional formation were confirmed by several experimental and numerical studies.[15–18] Results of an experimental study performed on granite rock samples demonstrated that increasing temperature, while the other fracturing parameters are kept constant, alters fractures' propagation direction and pattern inside the rock samples. Additionally, increase in temperature results in decrease in fracture initiation pressure, and the rock samples' mechanical properties (elastic moduli and compressive strengths).[19] Effects of temperature and confining pressure on dynamic elastic properties and permeability of the unconventional core samples were investigated in this experimental study.

2. Experimental procedure

To investigate effect of temperature on dynamic elastic properties of unconventional rock samples, eleven unsaturated outcrop core samples (four Barnett, four Eagleford, and three Wolfcamp) were used in this experimental study. Also, to study effect of temperature on permeability of the unconventional rock samples, seven outcrop core samples (three Wolfcamp, two Barnett and two Eagle Ford) were tested. The size of all core samples was 7.62 cm (3 in) length by 3.81 cm (1.5 in) diameter and they were dried in an oven at 100 °C to evaporate any existing free water.

A tri-axial cell, New England Research (NER) Autolab 1500, equipped with a furnace was used to measure the dynamic elastic properties and permeability of the samples at bottomhole conditions (Fig. 1).

This equipment can apply uniform confining pressure and axial load at elevated temperatures (up to 120 °C) and calculate dynamic elastic properties (Young's modulus and Poisson's ratio) by measuring velocities of P, S_1, and S_2 waves. Also, it can measure very low permeabilities (10 Nano Darcy (nD) to 500 micro Darcy (mD)).

To calculate the dynamic elastic moduli, P, S_1, and S_2 wave velocities were measured for each core sample and the results were then used to calculate bulk modulus, bulk compressibility, shear modulus, and Rickman's brittleness index using Eqs. (1) to (4).

$$G = \frac{\rho_b}{DTS^2} \tag{1}$$

$$K_b = \rho_b \left(\frac{1}{DTC^2} - \frac{4}{3DTS^2} \right) \tag{2}$$

$$C_b = \frac{1}{K_b} \tag{3}$$

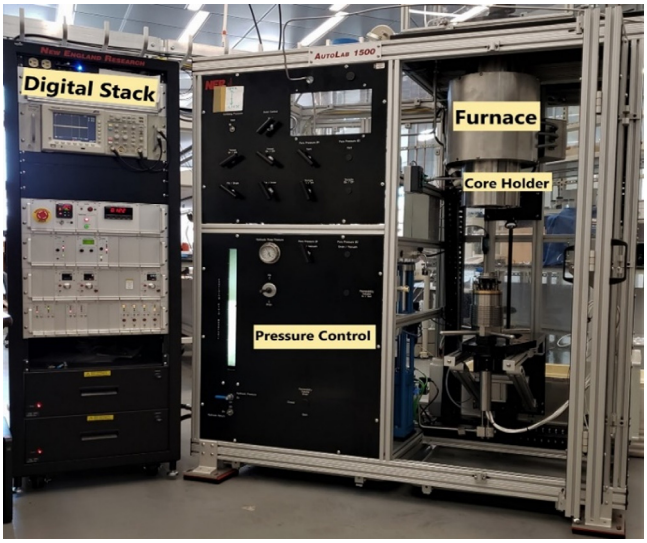

Fig. 1. NER autolab 1500 tri-axial cell.

$$\text{Rickman's Brittleness index} = \frac{50}{7}[E - 28\nu + 10.2] \tag{4}$$

where:
G: Shear modulus,
ρ_b: Bulk density,
DTS: Shear slowness,
DTC: Compressional slowness,
K_b: Bulk modulus
E: Young's modulus,
ν: Poisson's ratio
C_b: Bulk Compressibility

Special plugs capable of transmitting and receiving P, S_1, and S_2 waves were deployed to measure the waves' velocities. Each core sample was placed in a rubber sleeve and a wave transmitter plug (Source Plug) and a wave receiver plug (Receiver Plug) were then placed at the bottom and top of the core sample, respectively.

Fig. 2 illustrates a jacketed core sample mounted on the velocity measurement setup. Then, the setup was placed in the core holder and confining pressure was applied by pressurizing the mineral oil around the sleeve containing the core sample. The core holder temperature was controlled by the furnace.

Each core sample was tested at five different temperatures (20, 40, 60, 80, and 100 °C) and confining pressures (6.9, 13.8, 20.7, 27.6, and 34.5 MPa). P, S_1, and S_2 wave velocities were measured at each pairing of confining pressure and temperature and the results were then used to calculate the dynamic elastic properties.

Due to low permeability of the samples, transient pulse decay method was used to measure the permeability of the samples. Typical setup for pulse decay method is illustrated in Fig. 3.

To measure permeability of a core sample, the core sample is placed inside a rubber sleeve, isolating it from the confining fluid. The core sample is placed inside the core holder and the confining pressure, $P_c = 5.17$ MPa (750 psi), is applied to the core sample afterwards. All valves are open, and helium, as pore fluid, is injected into the core sample at a constant pressure, $P_o = 1.72$ MPa (250 psi), until the upstream and downstream pressures reach equilibrium. Then valve '1' is closed and the pressure of reservoir (V_1) slightly increases to P_1. Valve '1' is then opened and the pressure pulse slowly traverses through the core sample, decaying with time. Using two digital pressure

Fig. 2. Velocity measurement set up.

transducers, the core sample's upstream, P_u, and downstream, P_d, pressures were measured and recorded every two seconds until pressure equilibrium is reached ($P_u = P_d$). Then, using the following equations, the permeability of the sample is calculated from the slope of the straight line on a semi-log plot of $\Delta P(P_d - P_u)$ vs. time:

$$ln\frac{\Delta p(t)}{\Delta p_0} = -\alpha t \tag{5}$$

$$k = \frac{\alpha * \beta * \mu * L * V_{downstream}}{A} \tag{6}$$

where:
α: decay exponent
β: compressibility of the gas
μ: viscosity of the gas
L: length of core
$V_{downstream}$: volume of downstream reservoir
A: core cross sectional area

Permeability of each core sample was measured at five different temperatures: 20 °C (68 °F), 40 °C (104 °F), 60 °C (140 °F), 80 °C (176 °F), and 100 °C (212 °F). There are several methods to conduct pulse decay method and analyze the results. The ASPIKE pressure pulse, shown in Fig. 4, was used to measure the permeabilities of the samples in this study.

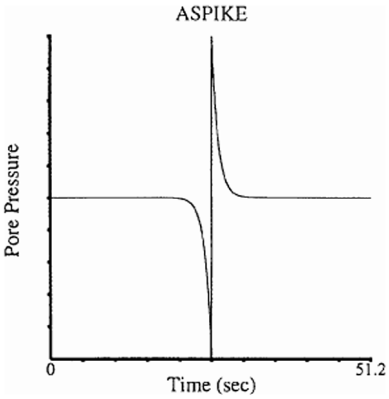

Fig. 4. ASPIKE pressure pulse method.

Fig. 5. Permeability measurement setup.

The core setup used to conduct the permeability measurement tests is depicted in Fig. 5. Mineralogy of the core samples were determined by implementing X-ray diffraction (XRD) analysis.

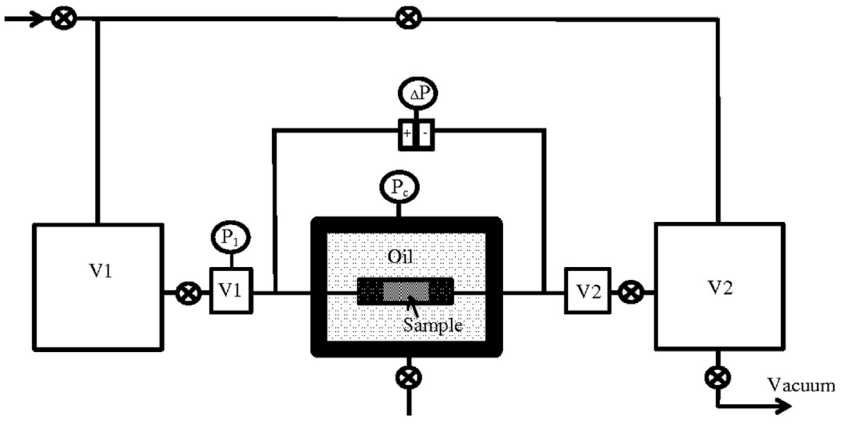

Fig. 3. Pulse decay permeability measurement setup (CoreLab).

Table 1
Change in wave velocities and dynamic elastic properties.

Core name	ΔVp (%)	ΔVs_1 (%)	ΔVs_2 (%)	ΔE (%)	$\Delta\upsilon$ (%)	ΔBI (%)
Wolfcamp						
W1-OC	1.2–2.8	1.6–2.3	2.2–2.4	3.5–4.6	0.35–1.7	3.8–4.1
W3-OC	1.6–2.8	1.7–2.4	2.2–2.7	4.3–5.5	0.3–1.7	4.2–4.6
W4-OC	0.9–1.9	1.1–1.9	1.25–2.3	3.8–4.9	0.4–1.6	3.9–5
Eagle Ford						
E1-OC	2.1–4.8	2.2–6.8	2.7–4.8	4.6–11	0.7–2.4	4.5–10.6
E2-OC	3.9–5	4.6–5.2	4.6–5.2	8.8–10	0.35–1.3	7.9–8.4
E3-OC	3–4.5	3.8–4.6	3.7–4.6	6.7–8.8	0.35–1.7	6.9–7.5
E4-OC	3.3–4.6	3.4–4.3	3.6–4.4	6.9–8.6	0.35–1.1	6.1–6.9
Barnett						
B1-OC	3.5–6.2	5.5–7.5	5.8–7.6	8.4–13.5	8.5–19.3	10.1–14.3
B2-OC	3.4–6.3	3.4–3.6	6.8–7.5	9–11.5	7.8–15.6	8.4–12.9
B3-OC	5.6–7.6	2.2–4.1	5.1–6.8	10.1–12.5	8.2–17.1	9.1–11.7
B4-OC	4.1–7.2	3.7–4.7	4.7–7.1	9.4–13.1	9.1–16.4	8.9–13.6

3. Results

3.1. Effects of temperature and confining pressure on rock dynamic elastic properties

For all eleven core samples (four Barnett, four Eagle Ford, and three Wolfcamp), the dynamic elastic properties were measured with similar results obtained for each basin. For each basin, the changes in wave velocities and consequently dynamic elastic properties with temperature and confined pressure were at the same range for each basin, shown in Table 1. Thus, for the sake of brevity, the results of one core sample from each basin are presented in this paper.

The results demonstrated that increasing confining pressure at a constant temperature results in increase in both compressional and shear wave velocities owing to the compaction of the core samples. On the other hand, increasing temperature at a constant confining pressure weakens the bonds between the grains and expands the rock matrix which decreases the waves' velocities. Using computed tomography (CT) scan images, Ref. 20 showed that increase in temperature results in creating new micro cracks and extending the existing ones that significantly increase the rock ductility. The degree of change in the velocities and consequently calculated dynamic elastic properties is directly related to mineralogy of a rock sample.

3.1.1. Wolfcamp core sample: W1-OC

The results of the XRD analysis revealed that the Wolfcamp core samples are merely composed of calcite and quartz. The core sample W1-OC is composed of 94.1%$_{wt}$ calcite and 5.9%$_{wt}$ quartz, shown in Fig. 6. Calcite ($CaCO_3$), a carbonate mineral, is a common constituent of sedimentary rocks, which its hardness on Mohs' scale is 3 (absolute hardness = 14). Quartz (SiO_4) is the most abundant and widely distributed mineral found at the Earth's surface and composed of silicon and oxygen. The hardness of quartz on Mohs' scale is 7 (absolute hardness = 100), which is seven times harder than calcite.

The Wolfcamp rock sample had high Young's modulus, 75.5 GPa. As shown in Figs. 7, 8, and 9, increasing temperature at each confining pressure resulted in decrease in P, S_1 and S_2 wave velocities owing to expansion of the matrix grains and creation of micro cracks in the rock matrix. Contrarily, increasing the confining pressure at each constant temperature resulted in reduction in the pore spaces owing to effect of compaction, which yields increase in the wave velocities throughout the rock matrix. Using the measured velocities and Eqs. (1) through (4), the dynamic elastic properties of the sample were calculated.

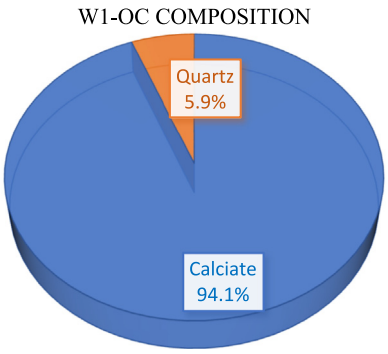

Fig. 6. W1-OC Composition, %$_{wt}$.

Hence, any change in the wave velocities resulted in change in the dynamic elastic properties.

The results demonstrated that increasing the confining pressure resulted in increase in the Young's modulus of the core sample by an average of 2%, while increasing the temperature caused decrease in the Young's modulus by an average of 4% (Fig. 10). The results show that temperature and confining pressure affect the rock stiffness in an opposite way and the effect of temperature is larger.

The results also demonstrated that effects of the confining pressure and temperature on the Poisson's ratio of the core sample are insignificant (Fig. 11).

Fig. 12 shows the effects of confining pressure and temperature on the bulk compressibility of the rock sample. The results demonstrate that bulk compressibility has a direct relationship with temperature and an inverse relationship with confining pressure. The results demonstrate that increasing the confining pressure from 7 MPa to 35 MPa at a constant temperature results in an average decrease of 3% in the bulk compressibility while increasing the temperature at a constant confining pressure causes an average increase of 4.5% in the bulk compressibility.

Using Eq. (4), Rickman's brittleness index of the sample was calculated at various confining pressures and temperatures and the results were plotted in Fig. 13. The results show that increasing the confining pressure results in negligible increase in the brittleness of the sample, while increasing the temperature makes the sample more ductile by lowering the brittleness index up to 4.5%. Despite increasing the confining pressure, the sample became more ductile at the elevated temperatures demonstrating the dominance of the effect of temperature.

3.1.2. Eagle Ford core sample: E1-OC

The results of the XRD analysis demonstrated that the Eagle Ford core sample E1-OC is composed of 92.6%$_{wt}$ Calcite, 5.9%$_{wt}$ Quartz, and 1.6%$_{wt}$ kaolinite, shown in Fig. 14. Kaolinite (Al2Si2O5(OH)4) is the most common clay mineral found on the earth with a soft consistency. Kaolinite is easily broken and can be easily molded or shaped, especially when wet. Kaolinite is brittle and its Mohs' hardness is 2–2.5 (absolute hardness = 2).

The results demonstrate that Young's modulus of the Eagle Ford core sample, 59.25 GPa, was lower than the Wolfcamp sample's owing to the presence of kaolinite. The results also demonstrated that increase in the temperature resulted in decrease in P, S_1, and S_2 wave velocities analogous to Wolfcamp sample (Figs. 15 through 20).

Akin to the previous results, at a constant temperature, increase in the confining pressure, from 7 MPa to 35 MPa, resulted in increase in the Young's modulus, about 5%, owing to the rock compaction (Fig. 15), whereas Poisson's ratio remained almost unchanged (Fig. 15). The results demonstrate that increase in

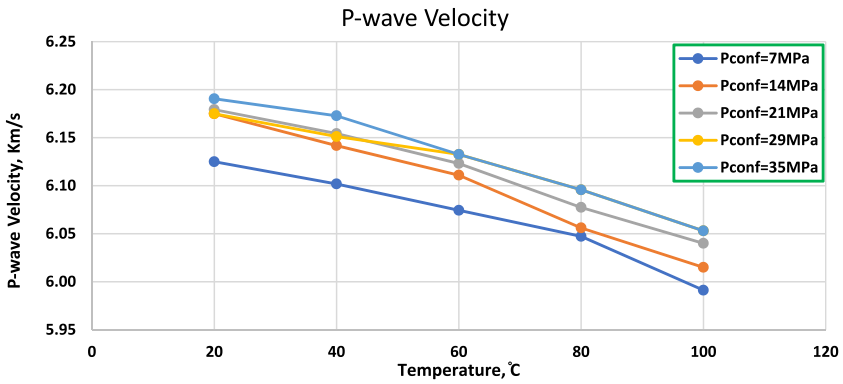

Fig. 7. P wave velocity vs. temperature for W1-OC.

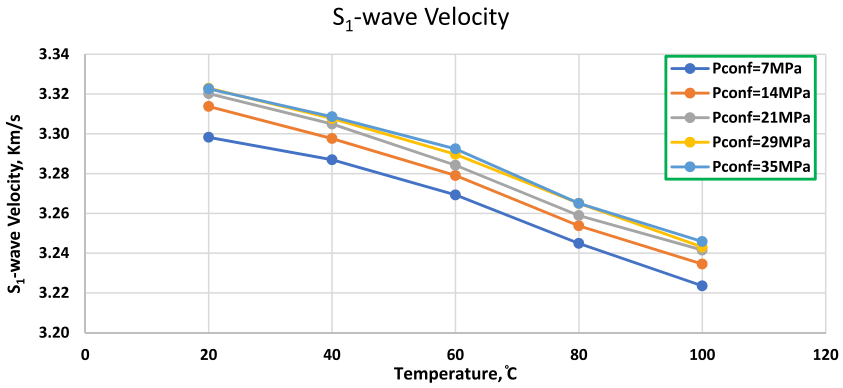

Fig. 8. S_1 velocity vs. temperature pressure, W1-OC.

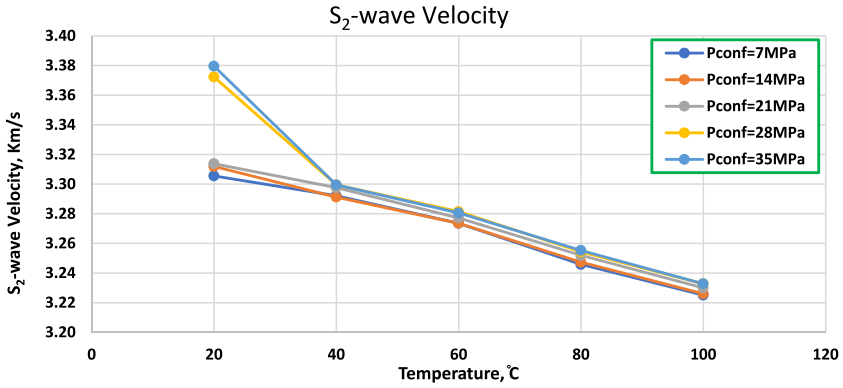

Fig. 9. S_2 velocity vs. temperature for W1-OC.

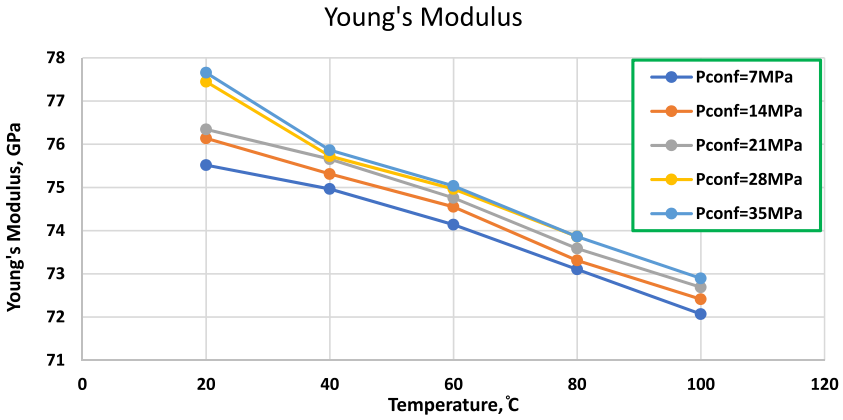

Fig. 10. Young's modulus vs. temperature, W1-OC.

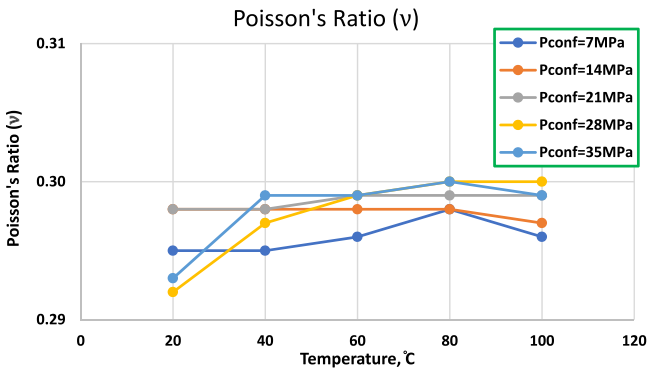

Fig. 11. Poisson's ratio vs. temperature, W1-OC.

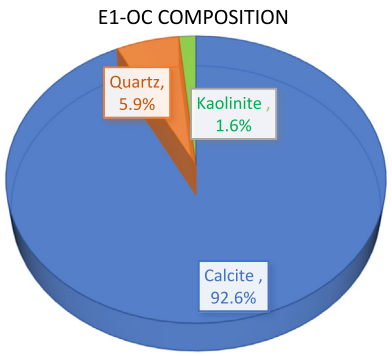

Fig. 14. E1-OC composition, %wt.

the temperature from 20 °C to 100 °C at a constant confining pressure, caused an average of approximately 10% decrease in the Young's modulus and made the rock more ductile (Fig. 15). It is worth noting that because of the presence of kaolinite, which is a ductile mineral, in the Eagle Ford sample, effect of the temperature on the its Young's modulus was more pronounced than the Wolfcamp sample's.

Fig. 12 shows the effects of confining pressure and temperature on the bulk compressibility of the rock sample. The results demonstrate the Eagle Ford core sample has a higher bulk compressibility than the Wolfcamp core sample owing to containing kaolinite. The results show that bulk compressibility has a direct relationship with temperature and an inverse relationship with confining pressure. Increase in confining pressure from 7 MPa to 35 MPa at a constant temperature results in an average decrease of 5% in the bulk compressibility while increasing the temperature at a constant confining pressure causes an average increase of 10% in the bulk compressibility. The results revealed that the effects of temperature and confining pressure on the bulk compressibility of this core sample is more pronounced than the previous core sample, Wolfcamp sample, because of the presence of the clay mineral, kaolinite.

Fig. 21 shows the brittleness index versus temperature at different confining pressures. At a constant temperature, increase in confining pressure resulted in an increase in brittleness of the sample by 3% because of compaction of the sample and increase in the Young's modulus, while increase in temperature lowered the rock stiffness and made the rock more ductile. The results clearly demonstrate that the effect of temperature on the brittleness index is dominant and at a constant confining pressure, increasing the temperature from 20 °C to 100 °C results in an average decrease of 7% in the brittleness index.

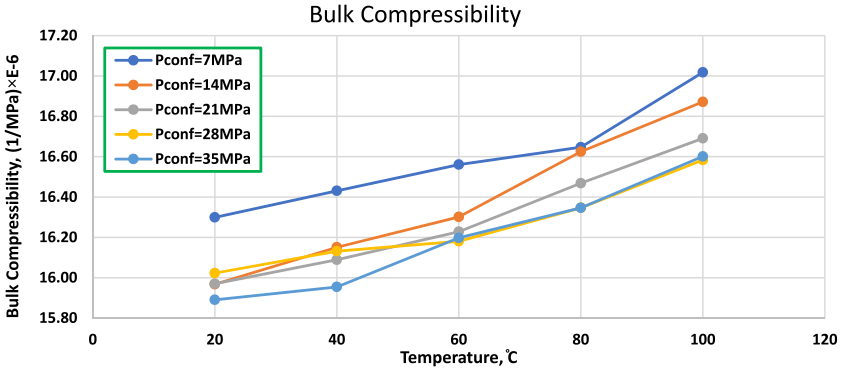

Fig. 12. Bulk compressibility vs. temperature, W1-OC.

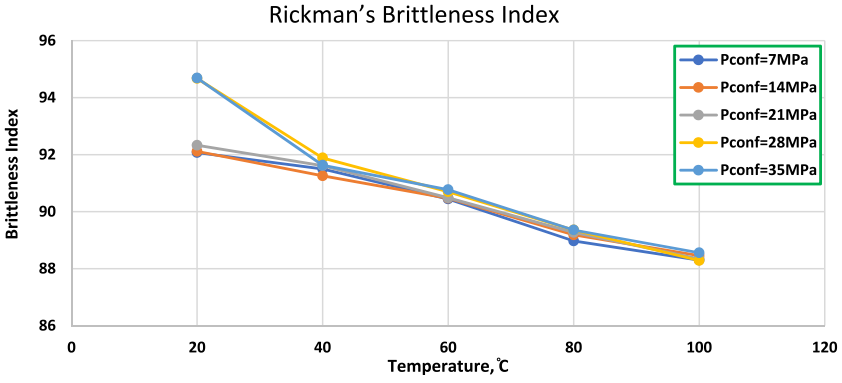

Fig. 13. Rickman's brittleness index vs. temperature, W1-OC.

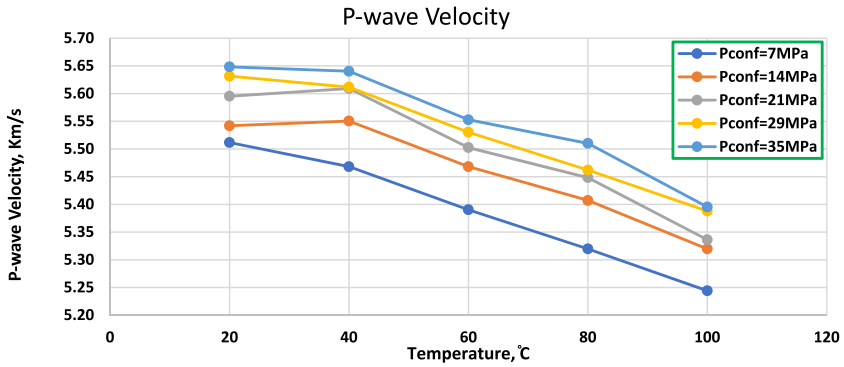

Fig. 15. P wave velocity vs. temperature, E1-OC.

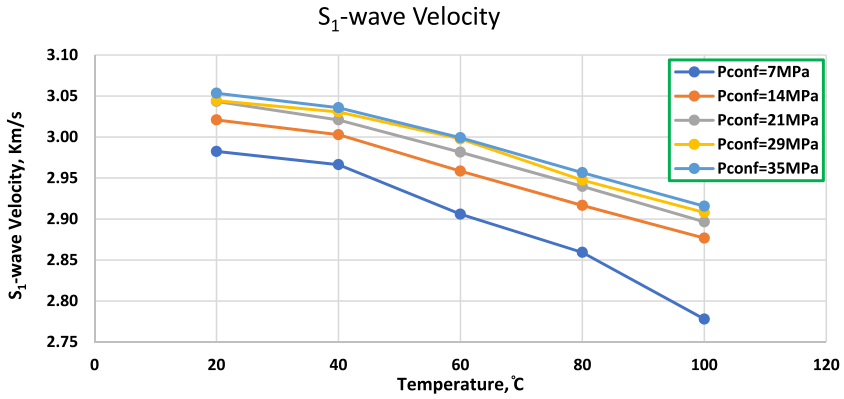

Fig. 16. S_1 wave velocity vs. temperature, E1-OC.

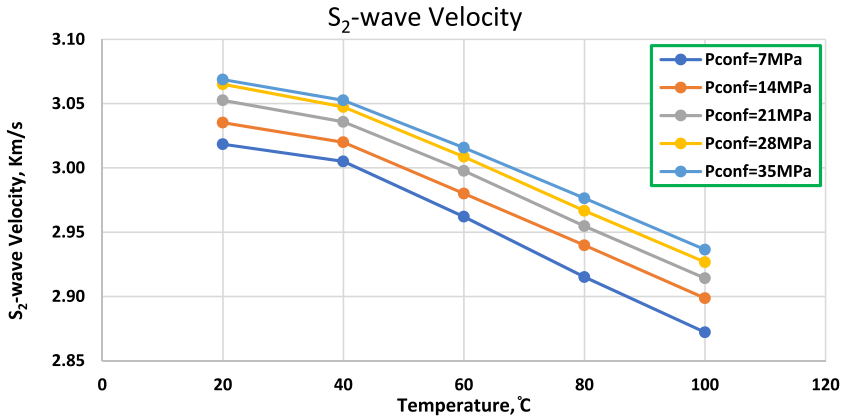

Fig. 17. S_2 wave velocity vs. temperature, E1-OC.

3.1.3. Barnett outcrop core sample: B1-OC

Barnett's core sample B1-OC is composed of quartz, pyrite, magnetite, halite, kaolinite, and illite, as shown in Fig. 22. Unlike the Wolfcamp and Eagle Ford core samples, calcite is absent in the composition of this core sample and is replaced by illite, magnetite, pyrite, and halite.

Illite $(K,H_3O)(Al,Mg,Fe)_2(Si,Al)_4O_{10}[(OH)_2,(H_2O)]$ occurs as an altered product of muscovite and feldspar in weathering and hydrothermal environments. It is common in sediments, soils, and argillaceous sedimentary rocks as well as in some low grade metamorphic rocks. Its Mohs' hardness is 1–2 (absolute hardness = 1–2). Magnetite (Fe_3O_4) is one of the iron ores and attracts magnet. Its hardness on Mohs' scale is 5.5–6.5 (absolute hardness = 48–72). Halite (NaCl), commonly known as rock salt, is a type of salt, the mineral form of sodium chloride, and its Mohs' hardness is 2.5 (absolute hardness = 8). Pyrite (FeS_2) is an iron sulfide and its Mohs' hardness is 6–6.5 (absolute hardness = 72–90).

The results demonstrate that the Barnett core sample has the lowest Young's modulus, 23 GPa, owing to its high clay content (48.7%). The initial P wave velocities in the Barnett rock sample were almost half of values in the Wolfcamp and Eagle Ford's cores, because of its high clay content and presence of existing visible cracks. P, S_1, and S_2 wave velocities decreased at elevated temperatures owing to the expansion of the rock micro-damages formed at elevated temperatures,[20] as shown in Figs. 23, 24, and 25. The results also demonstrate that increase in the confining pressure at a constant temperature caused increase in the waves velocities owing to the rock compaction. The results show that the effect of temperature on the waves velocities is dominant and

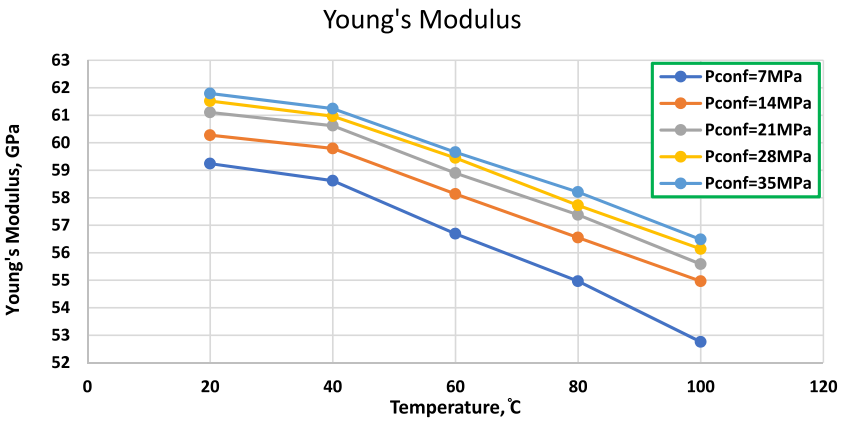

Fig. 18. Young's modulus vs. temperature, E1-OC.

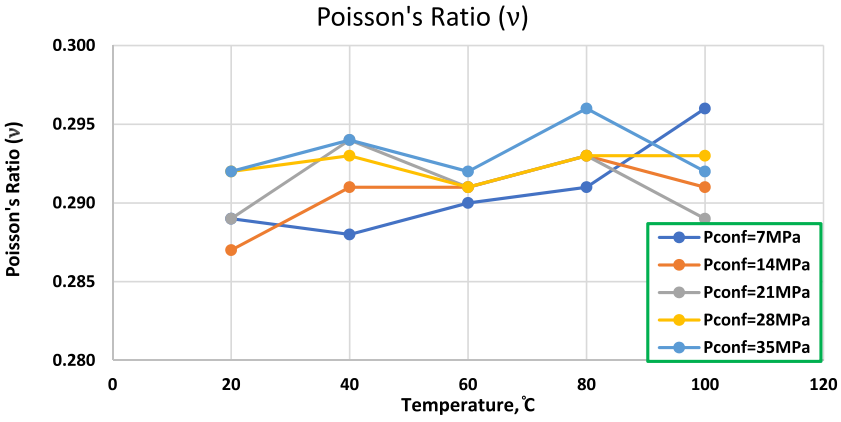

Fig. 19. Poisson's ratio vs. temperature, E1-OC.

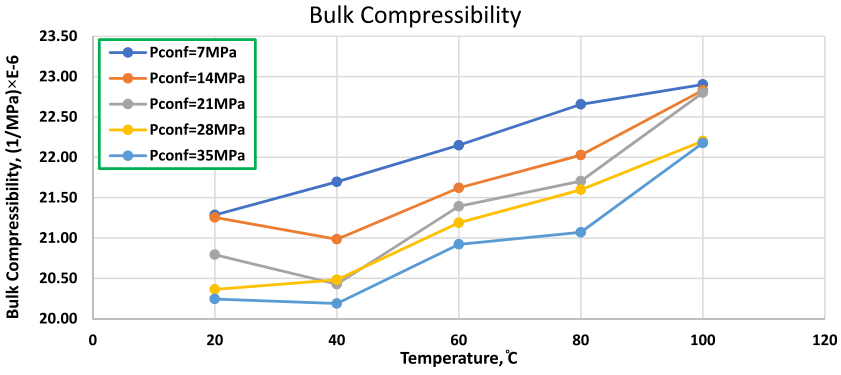

Fig. 20. Bulk compressibility vs. temperature, E1-OC.

the waves velocities decrease when both the temperature and confining pressure increase.

Fig. 26 demonstrates dynamic Young's modulus versus temperature at different confining pressures. The results show that at a constant temperature, increasing the confining pressure from 7 MPa to 35 MPa results in an average increase of 6% in the Young's modulus of the core sample. The results demonstrate that increase in temperature from 20 °C to 100 °C at a constant confining pressure resulted in an average decrease of 14% in the Young's modulus of the sample. It is worth noting that because of containing the highest clay content (48.7%), the highest reduction in Young's modulus due to the temperature increase happened in the Barnett core sample.

Unlike the Wolfcamp and Eagle Ford core samples in which the Poisson's ratios were almost independent of temperature, Poisson's ratio in Barnett's rock sample increased as temperature increased because of larger the change in the shear velocities due to high clay content (Fig. 27).

Fig. 28 shows the effects of confining pressure and temperature on the bulk compressibility of the rock sample. The results demonstrate that the highest bulk compressibility was observed in the Barnett core sample owing to having the highest clay content (48.7%). The results also demonstrate that increasing the confining pressure from 7 MPa to 35 MPa at a constant temperature results in an average decrease of 11% in the bulk compressibility while increasing the temperature at a constant confining pressure causes an average increase of 14% in the bulk

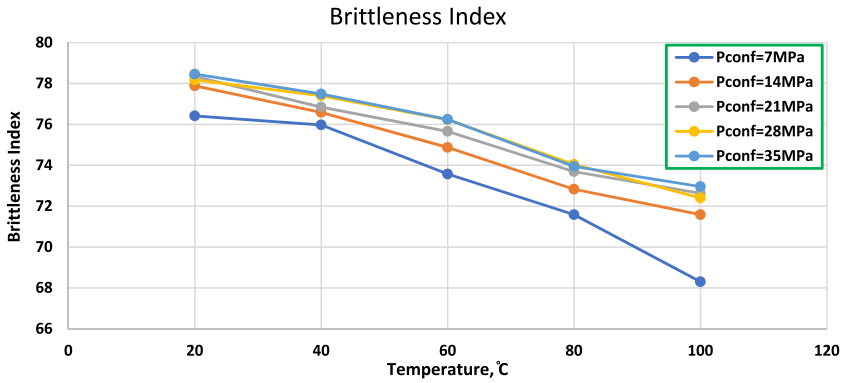

Fig. 21. Rickman's brittleness index vs, E1-OC.

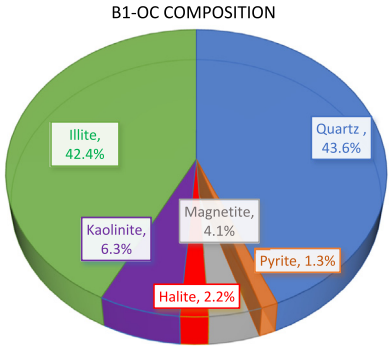

Fig. 22. B1-OC core sample mineralogical composition.

compressibility. The results revealed that the effects of temperature and confining pressure on the bulk compressibility of this core sample is more pronounced than the previous core samples, Wolfcamp and Eagle Ford samples, because of having the highest clay content.

Increase in the temperature results in a decrease in the Rickman's brittleness index indicating that the rock became more ductile at the elevated temperatures (Fig. 29). The results demonstrate that at a constant confining pressure, increase in the temperature from 20 °C to 100 °C results in an average decrease of 10% in the brittleness index. The reduction in the brittleness index was the highest in the Barnett core sample owing to containing the highest clay content.

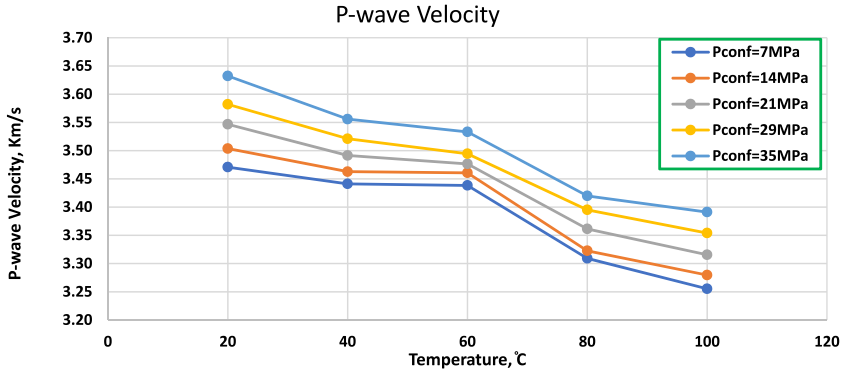

Fig. 23. P wave velocity vs. temperature, B1-OC.

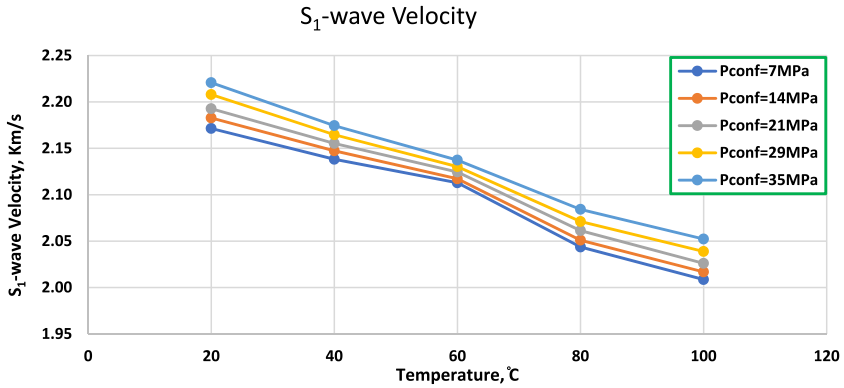

Fig. 24. S_1 wave velocity vs. temperature, B1-OC.

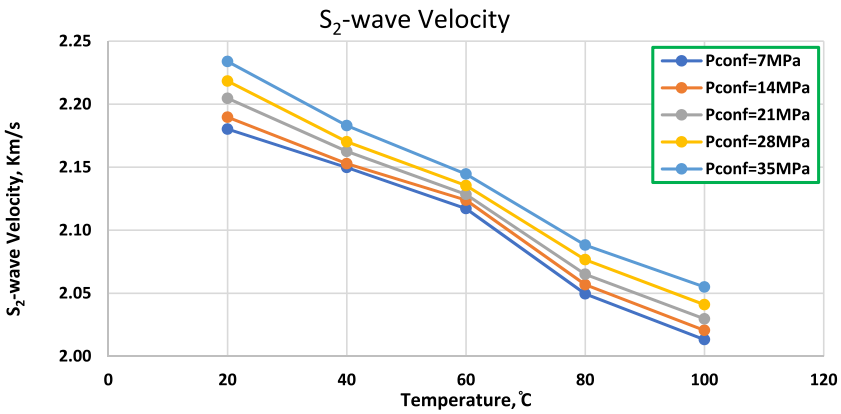

Fig. 25. S_2 wave velocity vs. temperature, B1-OC.

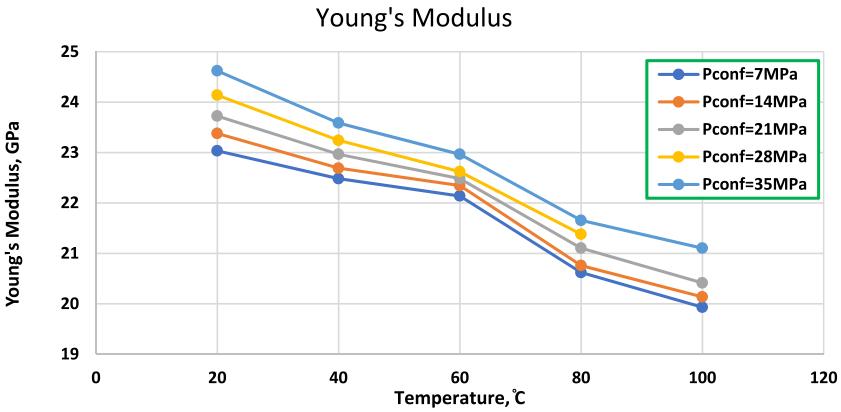

Fig. 26. Young's modulus vs. temperature, B1-OC.

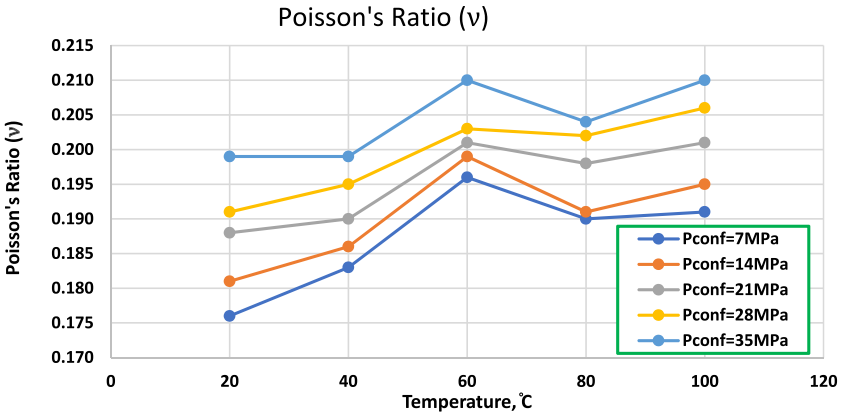

Fig. 27. Poisson's ratio vs. temperature, B1-OC.

3.2. Effect of temperature and confining pressure on the rock permeability

Permeability of seven core samples (two Barnett, two Eagle Ford, and three Wolfcamp) were measured at four different temperatures (20, 40, 60, 80 and 100 °C) and constant confining, 5.17 MPa (750 psi), and pore, 1.72 MPa (250 psi), pressures. Confining and pore pressures were chosen low to minimize their effects on the rocks' permeability measurements. Among the seven rock samples, core sample B2-OC (from Barnett basin) contained wide and visible cracks, resulting in very high initial permeability compared to the others (Fig. 30).

The results of the permeability measurements of the samples are presented in Table 2 and Fig. 31. The results demonstrate that increase in the temperature results in decrease in the permeability of all core samples, ranging from 77% to 99%, owing to expansion of the rock matrix and closure of the existing micro-cracks in the rock's body.

Since the permeability values for core sample B2-OC are substantially higher than the others, its values are shown in the right vertical axis (Fig. 31). Permeability decreases sharply beginning from 20 °C to 60 °C. From 60 °C to 100 °C, the effect is not as pronounced. Due to increase in the temperature, the grains in the rock matrix expand and occupy the pore spaces. This results in a decrease in the permeability. Most of the pore spaces

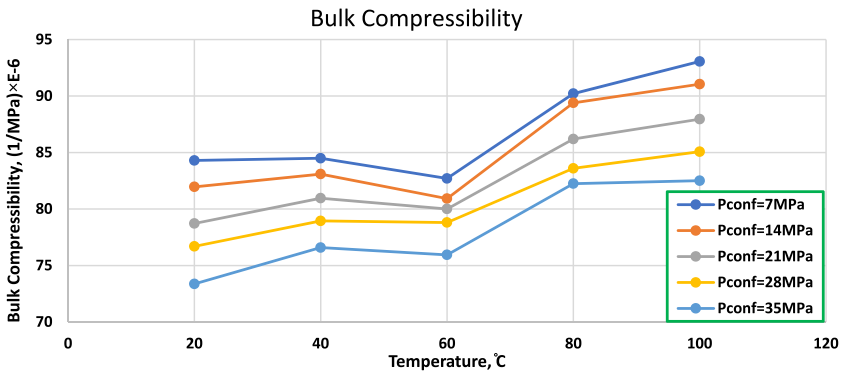

Fig. 28. Bulk compressibility vs. temperature, B1-OC.

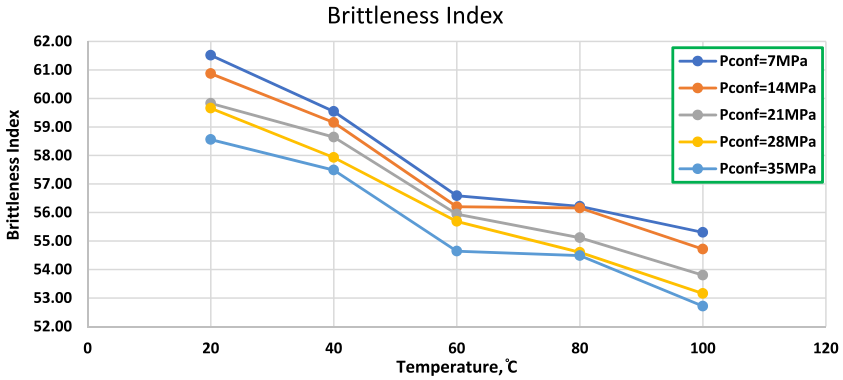

Fig. 29. Rickman's brittleness index vs. temperature, B1-OC.

Fig. 30. Core B2-OC containing wide cracks.

are occupied by expansion of the grains in the first stages of the temperature increase from 20 °C to 60 °C. Because of the confinement, majority of the pore spaces is utilized between 20 °C to 60 °C leaving less available pore spaces for expansion between 60 °C to 100 °C.

The results presented in Section 3.1 demonstrate that the Wolfcamp and Barnett samples had the highest and the lowest stiffness, respectively. Hence, the lowest and the highest permeability reduction occurred in the Wolfcamp and Barnett samples, respectively (Fig. 31).

4. Conclusions

The results of this experimental study demonstrate that the effects of temperature on the unconventional rock permeability and dynamic elastic properties: Young's modulus, brittleness index and bulk compressibility, are significant. The results show that increases in the confining pressure makes the rock sample more brittle, whilst increasing the temperature makes the rock ductile. The results also demonstrate that the effect of temperature on the rock brittleness index is more significant than the effects of the confining pressure. The results show that the degree of the effect of the temperature on the dynamic elastic properties of the samples is directly related to the presence and volume of the clay minerals. The results demonstrate that the highest reductions in Young's modulus, 14%, and brittleness index, 10%, were observed in the Barnett core samples because of having the highest clay content (48.7%). Whilst the lowest decreases in Young's modulus, 4%, and brittleness index, 5%, were observed in the Wolfcamp core samples owing to the absence of the clay minerals. Additionally, the results of the permeability tests show that temperature has a significant effect on the permeability of the core samples demonstrating that increasing the temperature significantly decreases the rock permeability. Since the matrix expansion is smaller in the stiff rock samples than the ductile rock samples, the effect of temperature on the permeability is less significant in the stiff core samples.

This experimental study was conducted on unsaturated outcrop core samples. It is recommended to investigate effects of temperature on the downhole core samples' dynamic elastic properties. It is also recommended to study effects of pore fluids and their saturations on the rock samples' dynamic elastic properties.

Table 2
Permeability vs. temperature.

Core sample	Temperature	20 °C	40 °C	60 °C	80 °C	100 °C
W1		5.97×10^{-3}	3.91×10^{-3}	1.36×10^{-3}	8.56×10^{-4}	7.12×10^{-4}
W3		3.7×10^{-4}	2.46×10^{-4}	1.35×10^{-4}	9.17×10^{-5}	8.26×10^{-5}
W4		2.24×10^{-3}	1.68×10^{-3}	1.13×10^{-4}	8.23×10^{-5}	5.84×10^{-5}
E1	Permeability, mD	1.16×10^{-2}	4.55×10^{-3}	1.15×10^{-3}	2.54×10^{-4}	1.12×10^{-4}
E4		6.68×10^{-3}	3.87×10^{-3}	2.46×10^{-3}	1.37×10^{-3}	5.08×10^{-4}
B2		11.3	1.27	0.907	0.877	0.237
B3		7.46×10^{-3}	4.85×10^{-3}	2.24×10^{-3}	1.06×10^{-3}	8.27×10^{-4}

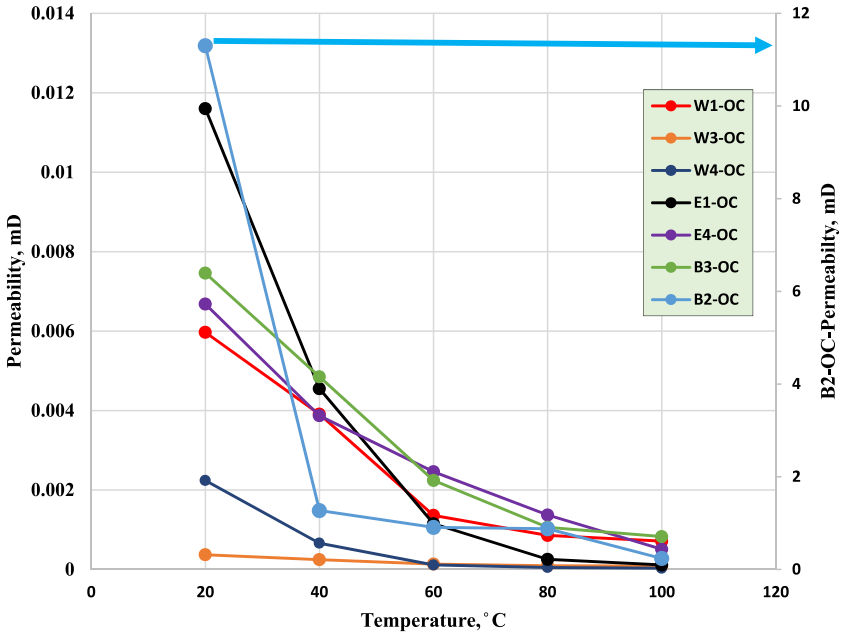

Fig. 31. Permeability vs. temperature at constant confining and pore pressures.

Declaration of competing interest

The authors declare that they have no known competing financial interests or personal relationships that could have appeared to influence the work reported in this paper.

References

1. Kolawole O, Ispas I. *How Hydraulic Fractures Interact with Natural Fractures: A Review and New Observations*. American Rock Mechanics Association; 2019.
2. Wigwe M, Kolawole O, Watson M, Ispas I, Li W. *Influence of Fracture Treatment Parameters on Hydraulic Fracturing Optimization in Unconventional Formations*. American Rock Mechanics Association; 2019.
3. Jin P, Hu Y, Shao J, Zhao G, Zhu X, Li C. Influence of different thermal cycling treatments on the physical, mechanical and transport properties of granite. *Geothermics*. 2019;78(March 2018):118–128. http://dx.doi.org/10.1016/j.geothermics.2018.12.008.
4. Oldakowski K, Sawatzky RP, Alvarez JM. Geomechanical properties of clear-water shale at elevated temperatures. In: *SPE Canada Heavy Oil Technical Conference*. 2016, http://dx.doi.org/10.2118/180694-MS, (June), 7–9.
5. Zamirian M, Aminian K, Ameri S. Measuring marcellus shale petrophysical properties. In: *SPE Western Regional Meeting*. 2016, http://dx.doi.org/10.2118/180366-MS.
6. Johnston DH. Physical properties of shale at temperature and pressure. *Geophysics*. 1987;52(10):1391–1401. http://dx.doi.org/10.1190/1.1442251.
7. Shao S, Ranjith PG, Wasantha PLP, Chen BK. Experimental and numerical studies on the mechanical behaviour of Australian strathbogie granite at high temperatures: An application to geothermal energy. *Geothermics*. 2015;54:96–108. http://dx.doi.org/10.1016/J.GEOTHERMICS.2014.11.005.
8. Ch.Lempp UB, Welte DH. The effect of temperature on rock mechanical properties and fracture mechanisms in source rocks - Experimental results. 1994.
9. Kumari WGP, Ranjith PG, Perera MSA, Shao S, Chen BK, Lashin A, … Rathnaweera TD. Mechanical behaviour of Australian Strathbogie granite under in-situ stress and temperature conditions: An application to geothermal energy extraction. *Geothermics*. 2017;65:44–59. http://dx.doi.org/10.1016/j.geothermics.2016.07.002.
10. Staudtmeister K, Zapf D, Leuger B, Elend M. Temperature induced fracturing of rock salt mass. *Procedia Eng*. 2017;191:967–974. http://dx.doi.org/10.1016/j.proeng.2017.05.268.
11. Brotóns V, Tomás R, Ivorra S, Alarcón JC. Temperature influence on the physical and mechanical properties of a porous rock: San Julian's calcarenite. *Eng Geol*. 2013;167:117–127. http://dx.doi.org/10.1016/j.enggeo.2013.10.012.
12. Yang S-Q, Tian W-L, Huang Y-H. Failure mechanical behavior of pre-holed granite specimens after elevated temperature treatment by particle flow code. *Geothermics*. 2018;72:124–137. http://dx.doi.org/10.1016/J.GEOTHERMICS.2017.10.018.
13. Kim KM, Kemeny J, et al. Effect of thermal shock and rapid unloading on mechanical rock properties. In: *43rd US Rock Mechanics Symposium & 4th US-Canada Rock Mechanics Symposium*. 2009, Retrieved from https://www.onepetro.org/conference-paper/ARMA-09-084.
14. Kumar DGM. *Effects of Temperature on Two Dimensional Hydraulic Fracturing in Impermeable Rocks*. American Rock Mechanics Association; 2011.
15. Ramezanian M, Emadi H, Elwegaa K. *An Experimental Study to Investigate the Effects of Temperature and Confining Pressure on Unconventional Rock Mechanical Properties*. American Rock Mechanics Association; 2019.
16. Soliman Mohammed, Wigwe Marshal, Ahmed Alzagabi EP. Analysis of fracturing pressure data in heterogeneous shale formations. *Hydraul Fract J*. 2014;1(2):8–14.
17. Elwegaa K, Emadi H. The effect of thermal shocking with nitrogen gas on the porosities, permeabilities, and rock mechanical properties of unconventional reservoirs. *Energies*. 2018;11(8):2131. http://dx.doi.org/10.3390/en11082131.
18. Elwegaa K, Emadi H, Ramezanian M. *Investigating Effects of Thermal Shock Technique on Unconventional Reservoir Rock Mechanical Properties*. American Rock Mechanics Association; 2019.

19. Zhou C, Wan Z, Zhang YGB. Experimental study on hydraulic fracturing of granite under thermal shock. *Geothermics*. 2018;71(1):146–155. http://dx.doi.org/10.1016/j.geothermics.2017.09.006.

20. Kim TW, Ross CM, Guan K, Burnham AK, Kovscek AR. Permeability and porosity evolution of organic rich shales as a result of heating. In: *SPE Western Regional Meeting*. Society of Petroleum Engineers: San Jose, California, USA; 2019, http://dx.doi.org/10.2118/195366-MS.